

High-pressure tuning of valence and magnetic interactions in $\text{Eu}_{0.5}\text{Yb}_{0.5}\text{Ga}_4$ G. D. Loula,¹ R. D. dos Reis,^{1,2} D. Haskel,³ F. Garcia,² N. M. Souza-Neto,^{2,*} and F. C. G. Gandra^{1,†}¹*Instituto de Física Gleb Wataghin, Universidade Estadual de Campinas (UNICAMP), São Paulo, Brazil*²*Laboratório Nacional de Luz Síncrotron, P.O. Box 6192, 13084-971, Campinas, São Paulo, Brazil*³*Advanced Photon Source, Argonne National Laboratory, Argonne, Illinois 60439, USA*

(Received 9 January 2012; revised manuscript received 20 March 2012; published 25 June 2012)

Pressure-induced changes in valence and magnetic ordering are observed in a $\text{Eu}_{0.5}\text{Yb}_{0.5}\text{Ga}_4$ compound by means of element selective x-ray absorption spectroscopy at Eu and Yb L_3 edges. Concomitant Eu and Yb valence transitions towards a $3+$ state, together with an antiferromagnetic to ferromagnetic transition, are observed with applied pressures up to 30 GPa. With the support of density functional theory calculations, we argue that hybridization between (Eu/Yb)- $5d$ and Ga orbitals regulates the valence and magnetic exchange interactions in this system.

DOI: [10.1103/PhysRevB.85.245128](https://doi.org/10.1103/PhysRevB.85.245128)

PACS number(s): 61.50.Ks, 75.20.Hr, 75.30.Mb, 71.70.Gm

I. INTRODUCTION

The EuGa_4 compound was discovered almost four decades ago and yet little is known about its electronic and magnetic properties today.^{1–3} It crystallizes in the tetragonal BaAl_4 structure with space group $I4/mmm$, where Eu planes are stacked between Ga planes. This arrangement results in a very stable structure in which Ga replacement is quite difficult to obtain.¹ However, the macroscopic physical properties of the compound can be modified if the electronic structure is altered. One possibility to achieve this is by a lattice contraction induced by chemical pressure (when Eu is substituted for another rare earth), or by application of external pressure.^{4–7} Among the few rare earth and related elements known to form the RGa compound, namely, $R = \text{La}, \text{Yb},$ and Sr ,¹ the use of Yb is particularly interesting because it does not fully comply with the nonmagnetic $2+$ configuration in YbGa_4 , as expected for the BaAl_4 structure. In a previous study of the series of compounds $(\text{Eu},\text{Yb})\text{Ga}_4$,² it was found that both magnetic moment and unit cell volume decrease as the Yb concentration increases from 0 to 1. X-ray absorption spectroscopy (XAS) experiments showed that all the samples display the presence of Yb^{2+} and Yb^{3+} so the magnetism was no longer simply due to the Eu^{2+} ions. Therefore, it would be interesting to investigate if an externally applied pressure, combined with the chemical pressure, would be able to drive the rare earth ions into a different valence and magnetic state.

In this paper we focus on the $\text{Eu}_{0.5}\text{Yb}_{0.5}\text{Ga}_4$ composition, because of its representativeness and simplicity when Eu and Yb are equally distributed in the lattice. This compound orders antiferromagnetically at $T_N = 13 \pm 0.3$ K with a saturated magnetic moment of $3.47 \pm 0.07 \mu_B$ (at $\mu_0 H \approx 70$ kOe) per formula unit (f.u.). This could be better understood if the lattice can be further contracted but without chemical alterations. Therefore, externally applied pressure was used to induce changes in the electronic structure of the Eu and Yb ions. We exploited the element and orbital selectivity of Eu and Yb L -edge x-ray absorption spectroscopy⁸ to probe the spin-polarized electronic structure of the $5d$ band states as the lattice is contracted under applied pressure in a diamond anvil cell (DAC). For both rare earth ions, valence changes were checked by x-ray absorption near edge structure (XANES) spectra, and the element specific magnetic

properties were probed by x-ray magnetic circular dichroism (XMCD). An $(\text{Eu}, \text{Yb})^{2+}$ to $(\text{Eu}, \text{Yb})^{3+}$ valence change and an antiferromagnetic (AFM) to ferromagnetic (FM) transition were induced by applied pressure. Our results, supported by density functional theory calculations, provide direct evidence that electronic hybridization effects are the leading mechanism that regulates the valence changes and magnetic ordering in this material. The complete spectroscopic description of the electronic structure and related changes in magnetism under pressure should guide efforts in understanding exchange interactions in similar rare earth intermetallic systems under lattice contraction.

II. METHODS

Single crystals of $\text{Eu}_{0.5}\text{Yb}_{0.5}\text{Ga}_4$ were prepared using the self-flux method in a 1:10 ratio compound f.u./Ga. Pure elements [rare earth (RE) 99.9%, Ga 99.99%] were placed inside an alumina crucible and sealed in a quartz ampoule with argon.¹ The ampoules were taken to a furnace and the temperature was raised to 950 °C at a 20 °C/min rate and remained at that temperature for 6 h. A slow rate of 0.1 °C/min was used to cool the samples down to 400 °C. The samples were subsequently centrifuged to separate the Ga flux and were further mechanically cleaned to remove any excess Ga. This process provided platelike crystals with typical dimensions of $5 \times 5 \times 2$ mm. Magnetic properties were measured in a Quantum Design superconducting quantum interference device (SQUID) magnetometer.

X-ray absorption near edge structure (XANES) and x-ray magnetic circular dichroism (XMCD) measurements at the Eu and Yb L_3 edges and Ga K edge were carried out in transmission geometry at beamline 4-ID-D of the Advanced Photon Source, Argonne National Laboratory. The beamline is equipped with phase-retarding optics to convert the linear polarization of synchrotron radiation to circular.⁹ The XMCD spectra are obtained from measurements of the helicity-dependent absorption coefficient $\mu^{+,-}$, normalized by the absorption edge jump as $(\mu^+ - \mu^-)$ while the spin-averaged XANES is defined as $(\mu^+ + \mu^-)/2$. The XMCD measurements were performed for two directions of the applied magnetic field, along and opposite the incident photon wave vector, to check for systematic errors. We used a He-flow

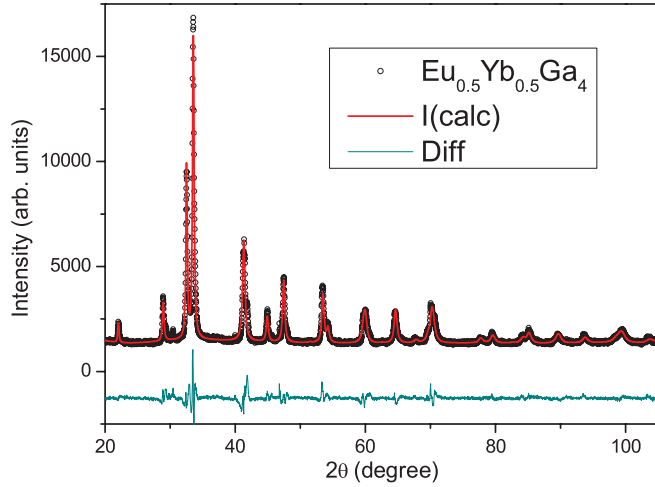


FIG. 1. (Color online) X-ray diffractogram of a powdered $\text{Eu}_{0.5}\text{Yb}_{0.5}\text{Ga}_4$ single crystal at 300 K and ambient pressure.

cryostat able to reach temperatures as low as 3 K which inserts into the bore of a split-coil superconducting magnet that is capable of reaching a ± 4 T magnetic field. Although $(\text{Eu},\text{Yb})\text{Ga}_4$ is antiferromagnetic at ambient pressure, the 4 T applied magnetic field is high enough to induce a ferromagnetic component of Eu spins, producing a net magnetic moment to be probed by XMCD.

To reach pressures as high as 30 GPa we used a nonmagnetic, miniature diamond anvil cell (mini-DAC) manufactured by D'anvils using partially perforated diamond anvils with 300 μm culets.¹⁰ The total diamond thickness in the x-ray's path was 1.8 mm, minimizing x-ray attenuation and enabling the measurements at the relatively low energy of the Eu L_3 edge (6.97 keV). A nonmagnetic 316 stainless-steel gasket, 250 μm thick, was preindented to 40 μm and a 140 μm hole was made in the center as a sample chamber. Silicone oil was used as the pressure transmitting medium. A powdered crystal sieved down to 20 μm was well mixed with the silicone oil and loaded into the gasket hole. The pressure was applied at ambient temperature and calibrated using the ruby luminescence method.¹¹ When cooled to low temperature no change in pressure was detected within a ± 1 GPa error bar,

as determined by independent x-ray absorption fine structure (XAFS) measurements on Cu powders.¹²

Density functional theory *ab initio* calculations were performed using the WIEN2K implementation of the full-potential linearized augmented plane-wave (APW) method with a double-counting scheme and the rotationally invariant local density approximation (LDA) + U functional with $U = 7$ eV.¹³ The size of APW + local orbital (lo) basis was determined by the cutoff $R_{\text{mt}}K_{\text{max}} = 8$, with 99 irreducible k points out of a 1000 k -point regular grid in the Brillouin zone. Only ferromagnetic structures were considered and spin-orbit coupling was neglected.

III. AMBIENT PRESSURE CHARACTERIZATION

EuGa_4 crystallizes with the BaAl_4 structure¹ and so does $\text{Eu}_{0.5}\text{Yb}_{0.5}\text{Ga}_4$. Although lattice parameter a shows a contraction of about 0.25%, lattice parameter c increases nearly 0.15% relative to the parent compound. The x-ray diffractogram and the correspondent calculated one for the $\text{Eu}_{0.5}\text{Yb}_{0.5}\text{Ga}_4$ sample are shown in Fig. 1 with the Rietveld refinement results presented in Table I. A small amount of Ga excess flux was detected and related to the extra peak near 31° in the as-grown samples. Although this nonmagnetic, metallic Ga impurity phase does not affect the XMCD results, extra care was taken in preparing samples for XANES/XMCD measurements by cleaning the material's surface to minimize the presence of Ga flux. In addition to the x-ray diffraction assessment of the crystalline phase, we used the ratio of the Eu and Yb L_3 absorption edge jumps to determine the sample composition with about 1% precision. We determined $x = 0.49$ instead of a nominal value $x = 0.5$ for the $\text{Eu}_x\text{Yb}_{1-x}\text{Ga}_4$ sample.

The magnetization for $\text{Eu}_{0.5}\text{Yb}_{0.5}\text{Ga}_4$ is presented in Fig. 2, together with the results for EuGa_4 and YbGa_4 . The Néel temperature, the saturation field, and the saturated moment decrease with inclusion of Yb. This behavior is consistent with a reduction of the Eu exchange interaction assuming Yb enters the lattice as a nonmagnetic ion. However, from our preliminary XANES results, we show that at least part of the Yb content in $\text{Eu}_{0.5}\text{Yb}_{0.5}\text{Ga}_4$ is magnetic, resulting in a more complex situation. Because conventional magnetization

TABLE I. Rietveld refinement results for $\text{Eu}_{0.5}\text{Yb}_{0.5}\text{Ga}_4$ and EuGa_4 . Both compounds crystallize in the tetragonal BaAl_4 structure with space group $I4/mmm$.

Lattice parameters	$\text{Eu}_{0.5}\text{Yb}_{0.5}\text{Ga}_4$	EuGa_4			
a, b (Å)	4.3872(2)	4.4006			
c (Å)	10.6900(6)	10.6739			
α (Å)	90	90			
β (Å)	90	90			
γ (Å)	90	90			
V (10^6 pm^3)	205.758	206.704			
Occupancy, atomic fractional coordinates for $\text{Eu}_{0.5}\text{Yb}_{0.5}\text{Ga}_4$					
Atom	Site	Occupancy	x	y	z
Eu1	2a	0.500000	0.000000	0.000000	0.000000
Yb1	2a	0.500000	0.000000	0.000000	0.000000
Ga1	4d	1.000000	0.000000	0.500000	0.250000
Ga2	4e	1.000000	0.000000	0.000000	0.3834(3)

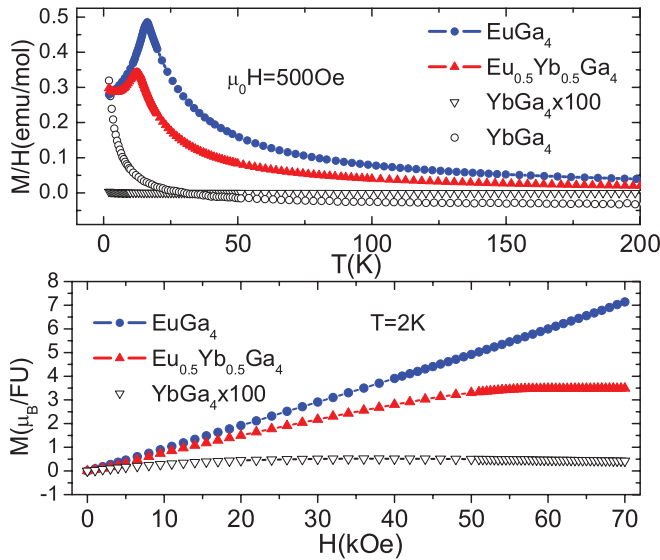


FIG. 2. (Color online) Magnetization of $\text{Eu}_{0.5}\text{Yb}_{0.5}\text{Ga}_4$ vs temperature (upper panel) and magnetic field (lower panel). We also show the results for EuGa_4 and YbGa_4 for comparison.

measurements can only assess the global magnetic properties of the sample, a microscopic description of the properties of each atomic species can be elucidating. This can be provided by XANES and XMCD measurements, which we present below.

IV. EUROPIUM L_3 XANES/XMCD UNDER PRESSURE

We used the element and orbital selectivity of x-ray absorption spectroscopy in the dipolar ($2p \rightarrow 5d$)⁸ and quadrupolar ($2p \rightarrow 4f$)^{14,15} channels to independently probe the electronic configuration of Eu and Yb ions. Looking at XANES spectra it is easy to identify the contribution from Eu^{2+} ($5d^0 4f^7$) and Eu^{3+} ($5d^1 4f^6$) since their threshold energies are separated by 8.5 eV due to the different Coulomb repulsion. The XANES and XMCD measurements at the Eu L_3 edge (6.97 eV) for a $\text{Eu}_{0.5}\text{Yb}_{0.5}\text{Ga}_4$ sample under pressure are shown in Fig. 3. We observe that the external pressure induced a decrease of the Eu^{2+} content with a concomitant increase of the Eu^{3+} contribution, evidencing an expected valence change. We also note that the spectral weight from the Eu^{2+} peak is only partially transferred to the Eu^{3+} peak at high pressures, which is likely an indication of $5d$ band hybridization effects.

Using the spin-dependent sensitivity and atomic selectivity of XMCD we can separately probe the magnetic properties for each ion (Eu or Yb, 2+ and 3+) under high pressures. In a similar fashion to the spin-averaged XANES, XMCD spectra probe the spin-dependent density of states (DOS) near the Fermi level. Therefore, we must keep in mind that the gradual filling of the $5d$ (initially empty states) as a function of the applied pressure, evidenced in the XANES spectra, also affects the amplitude of the XMCD.

Figure 3 presents the XMCD spectra for the $\text{Eu}_{0.5}\text{Yb}_{0.5}\text{Ga}_4$ sample as a function of the applied pressure. While the Eu^{3+} contribution (due to its $4f^6$ weak Van Vleck paramagnetism) is mostly negligible, the Eu^{2+} strong magnetic signal is drastically affected by pressure. The amplitude of the XMCD

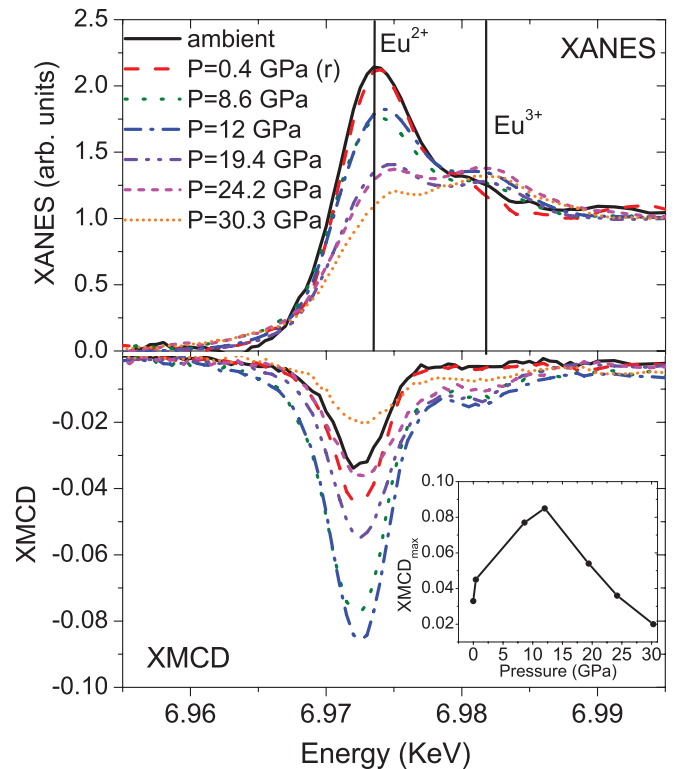


FIG. 3. (Color online) Europium L_3 XANES and XMCD spectra obtained at $T = 6$ K and $\mu_0 H = 4$ T for a powdered sample as a function of applied pressure. The characteristic XANES peaks of Eu^{2+} and Eu^{3+} are identified. (r) indicates measurement done after pressure release. Inset: XMCD peak amplitude as a function of applied pressure.

signal significantly increases up to 12 GPa and then decreases for higher pressures (see the inset of Fig. 3). In addition to these observed changes in the magnitude of the Eu ferromagnetic component, pressure also induces an increase in the magnetic ordering temperature, as revealed in Fig. 4. Both effects (an increase in ordering temperature and magnitude of the FM component) appear to be at odds with the response of the samples to chemical pressure seen in the conventional magnetization measurements (Yb doped and undoped; see Fig. 2).

We now focus on the field dependence of the XMCD peak amplitude as a function of pressure: Magnetization loops plotted in Fig. 5 unquestionably show an antiferromagnetic to ferromagnetic transition induced by pressure. The coercive field continuously increases up to 30 GPa (the inset of Fig. 5), indicating that ferromagnetic interactions are strengthened by lattice contraction. This is not surprising since other europium based compounds have been shown to present ferromagnetic ordering enhancement under chemical and applied pressures.^{16,17}

As described above, the observed pressure dependences of XMCD amplitude, ordering temperature, and coercive field unequivocally show that the europium magnetic interactions are drastically affected by lattice contraction, as do the overall electronic properties of the compound. A possible mechanism to explain these effects is a simple mean-field treatment of carrier-mediated coupling described by Ruderman-Kittel-

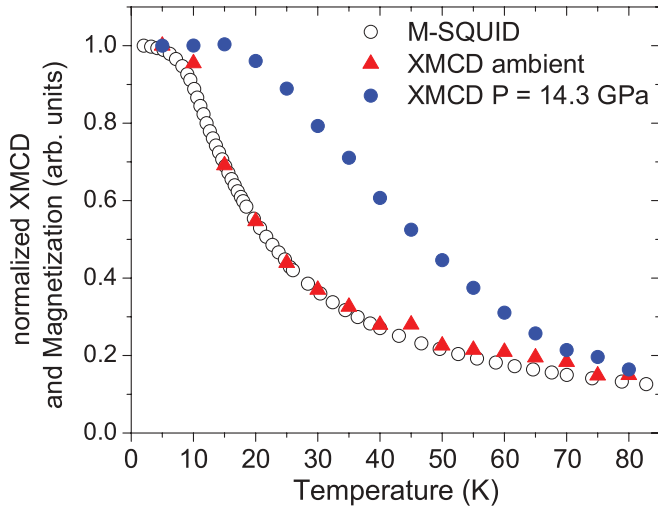


FIG. 4. (Color online) Europium L_3 -edge XMCD peak amplitude obtained at 4 T for ambient pressure and 4 GPa as a function of the temperature. For a comparison we also plotted the magnetization obtained in a SQUID magnetometer and all the curves were normalized at lowest temperature.

Kasuya-Yoshida (RKKY) interactions. In this scenario the interplanar interactions are mediated by conduction electrons from Ga atoms that are stacked between Eu-Yb planes in the compound. We must consider that the strength of RKKY coupling oscillates and decays^{18–21} as a function of the distance between the Eu planes. Then it is likely that the transition from AFM to FM ordering and the related increase in ordering temperature is related to the switch in sign of the RKKY coupling, together with an increased overlap of Eu/Yb- $5d$ and Ga orbitals under pressure. The decrease in XMCD signal at higher pressures is likely a result of a significant decrease in the fraction of Eu^{2+} magnetic ions between 12 and 19 GPa (Fig. 3) without a concomitant increase in the fraction of magnetic Yb^{3+} ions in this pressure range (Fig. 8), resulting in a dilution

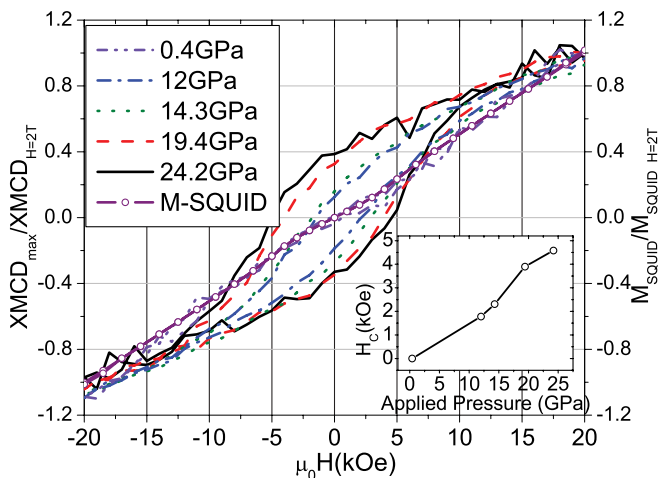


FIG. 5. (Color online) Hysteresis curves of the Eu L_3 XMCD peak amplitude as a function of applied pressure. For comparison we show the magnetization at ambient pressure obtained in a SQUID magnetometer. Inset: Coercive vs pressure. All data were taken at $T = 6$ K.

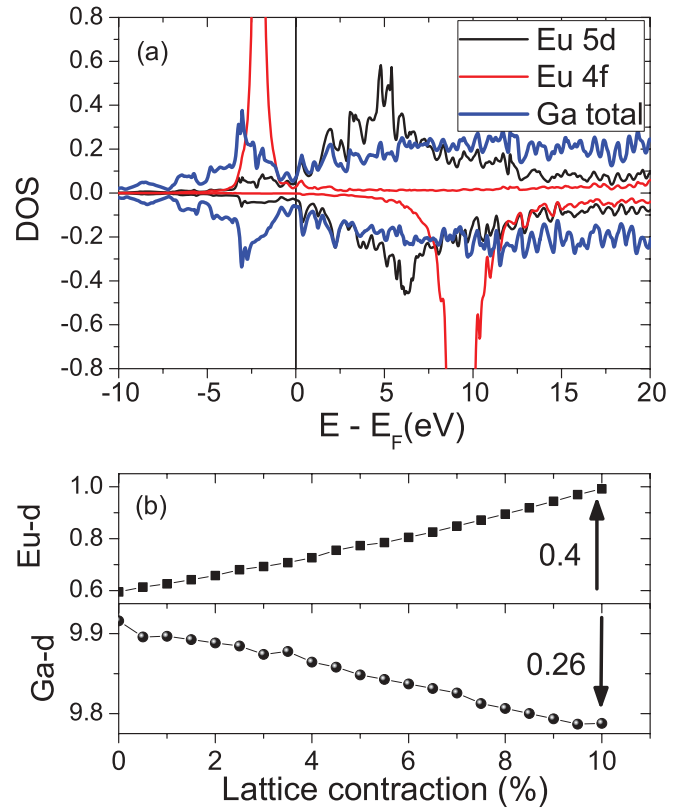


FIG. 6. (Color online) (a) Calculated density of states for Eu $5d, 4f$ orbitals and Ga total DOS showing electronic hybridization between Eu- $5d$ and Ga orbitals. (b) Electronic occupation numbers for Eu- $5d$ and Ga- $3d$ as a function of lattice contraction. The simulations were done on the parent compound EuGa_4 .

of magnetic interactions. Unlike physical pressure, Yb doping forces a dilution of the Eu magnetic ions, therefore weakening the magnetic interactions, and consequently reducing the ordering temperature and saturation moment. We note that, while Yb doping contracts the in-plane lattice parameter (chemical pressure), it expands the c axis (Table I). The latter would contribute to a reduction in the strength of interplanar RKKY interactions.

V. ELECTRONIC HYBRIDIZATION EFFECTS

With the goal of pinpointing the relevant spin-dependent electronic changes that regulate the observed valence and magnetic properties as a function of pressure, we performed *ab initio* LDA + U calculations of the orbital-dependent density of states and electronic occupations as a function of lattice contraction on EuGa_4 . The results summarized in Fig. 6 show a strong hybridization between Eu- $5d$ and gallium orbitals. This is evidenced by the increase of Eu- $5d$ occupation concomitant with the decrease of Ga- $3d/4p$ occupation and by the strong overlap between Eu- $5d$ and Ga density of states. In addition to that, an increase in the interstitial charge occupation (defined as the charge outside the muffin-tin sphere) indicates that more electronic states are shared by all atomic species of the material. This scenario reinforces the arguments that RKKY-like magnetic interactions are enhanced, together with changes in superexchange interactions mediated by nonmagnetic Ga

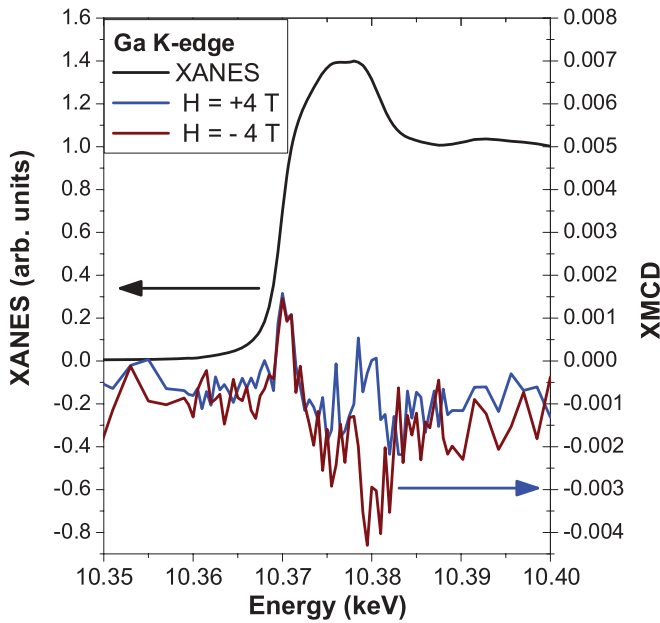


FIG. 7. (Color online) Ga K -edge XANES and XMCD spectra of $\text{Eu}_{0.5}\text{Yb}_{0.5}\text{Ga}_4$ measured at a temperature (T) of 3 K and 4 T magnetic field. XMCD is plotted for both field directions (± 4 T) to account for artifact effects in the polarization-switching mode. The XMCD signal is evidenced by the sign switching of the spectra measured with $+4$ and -4 T applied magnetic field.

atoms. The competition between these interactions and the change in valence of Eu will inevitably regulate the magnetic ordering properties of the compound as a function of pressure.

In view of the LDA + U results, one would expect some induced magnetism to be present at Ga states in a similar fashion to the observed Ge polarized states in $\text{Gd}_5\text{Si}_2\text{Ge}_2$.²² To verify this we measured Ga K -edge XMCD on $\text{Eu}_{0.5}\text{Yb}_{0.5}\text{Ga}_4$ shown in Fig. 7, which indeed presents a weak magnetic signal in the Ga $4p$ states. While XMCD signals in magnetic ions are usually largest at, or near, the absorption threshold, the spin-dependent signal at the Ga K edge is largest 10 eV above the edge. Based on the density of states determined by LDA + U (Fig. 6), it appears that this XMCD signal originates in the hybridization of Ga orbitals with Eu $4f$ minority states (at 10 eV above the Fermi level) and the Eu $5d$ band; i.e., it is an induced polarization. The strong hybridization between Eu $5d$ and Ga orbitals near the Fermi energy affects the long-range exchange interaction between Eu ions.

VI. YTTERBIUM L_3 XANES/XMCD UNDER PRESSURE

Considering that ytterbium is known to present mixed valence behavior in some materials, we performed Yb L_3 -edge XANES measurements to check the pressure dependence of the Yb valence on $\text{Eu}_{0.5}\text{Yb}_{0.5}\text{Ga}_4$. As expected, we observed an increase in Yb^{3+} ($4f^{13}$) states at the expense of Yb^{2+} ($4f^{14}$) states as a function of pressure (Fig. 8), in a similar fashion to the Eu valence change. This mixed valence behavior of Yb ions, even at ambient pressure, is in disagreement with the assumption that the total moment of the compound seen in magnetization measurements is predominantly due to europium ions, since Eu^{2+} and Yb^{3+} both carry a magnetic

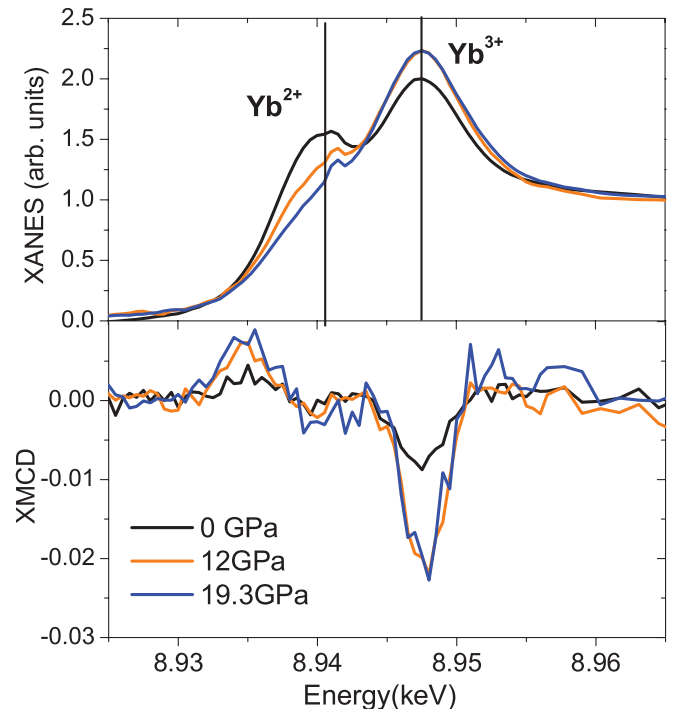


FIG. 8. (Color online) Ytterbium L_3 -edge XANES and XMCD spectra measured at $T = 6$ K, 4 T applied magnetic field, and as a function of applied pressure. Yb^{2+} and Yb^{3+} characteristic XANES peaks are identified.

moment. Motivated by these aspects we performed XMCD measurements at the Yb L_3 edge (shown in Fig. 8). We observed that Yb indeed carries a sizable magnetic moment, which has the same sign of the Eu XMCD signal, therefore indicating ferromagnetic alignment of Yb and Eu moments. Moreover, as pressure is applied, the moment increases concomitant with the increase of the Yb^{3+} magnetic ion contribution from XANES and the increase of the Eu XMCD amplitude signal. These results conclusively show that the magnetic moment of the compound is not only due to Eu ions, as one would assume when only bulk measurements were available.

Interestingly, we observe an unexpectedly small XMCD peak in the pre-edge. One could speculate it is due to a magnetic moment from the Yb^{2+} contribution, however, this interpretation would conflict with the atomic model that a $4f^{14}$ ion is inherently nonmagnetic. In addition to that, the Yb^{2+} contribution determined by XANES decreases with applied pressure, in opposition to the XMCD pre-edge peak, which increases with pressure. Nevertheless, this can be expected if the strong hybridization promoted by pressure is inducing a stable quantum state of Yb^{2+} valence but with fractional $4f$ occupation (e.g., $4f^{13.9}$). Another interpretation for this small pre-edge peak would be that it is due to a quadrupolar ($2p \rightarrow 4f$) contribution to the Yb^{3+} ($4f^{13}$) cross section, however, the large energy difference of about 13 eV between the two XMCD peaks makes this scenario unlikely. The origin of this pre-edge peak in the Yb XMCD signal is still a matter of debate and further investigations are needed to clarify its origin.

VII. SUMMARY

In summary, we used the element and orbital selectivity of XANES and XMCD measurements on Eu and Yb L_3 absorption edges to probe the valence and magnetic properties of the compound $\text{Eu}_{0.5}\text{Yb}_{0.5}\text{Ga}_4$ under pressures of up to 30 GPa. We showed that both the Eu and Yb sublattices are magnetic. The valence of both Eu and Yb changes towards $3+$ as pressure is increased, concomitant with changes in magnetic ordering. An enhancement of the ordering temperature and magnetic moment in both sublattices, as well as an antiferromagnetic to ferromagnetic order transition clearly observed at high pressures, are attributed to changes in the RKKY magnetic interactions induced by applied pressure. With the support of density functional theory and Ga K -edge XMCD, we argue that a strong hybridization between Eu- $5d$ and Ga bands is the relevant electronic mechanism that regulates the changes in indirect exchange interactions (RKKY and superexchange).

A small pre-edge peak in the XMCD of Yb was observed and its origin will remain a matter of discussion in future investigations to determine if it is due to induced $5d$ magnetism in nonmagnetic Yb^{2+} ions or due to an Yb^{3+} quadrupolar $4f$ contribution. This complete spectroscopic study of electronic structure and magnetic changes under pressure should guide efforts in understanding exchange interactions in similar rare earth intermetallic systems under lattice contraction.

ACKNOWLEDGMENTS

We thank L. P. Cardoso for the x-ray diffraction data and Antonio Medina and Luzeli M. da Silva for fruitful discussions. We acknowledge financial support from the Brazilian agencies CNPq, CAPES, and FAPESP. Work at Argonne is supported by the US Department of Energy, Office of Science, Office of Basic Energy Sciences, under Contract No. DE-AC-02-06CH11357.

*narcizo.souza@lnls.br

†gandra@ifi.unicamp.br

¹S. Bobev, E. D. Bauer, J. Thompson, and J. L. Sarrao, *J. Magn. Mater.* **277**, 236 (2004).

²G. Loula, L. da Silva, A. dos Santos, A. Medina, and F. Gandra, *Physica B: Condens. Matter* **403**, 946 (2008).

³J. D. Vries, R. Thiel, and K. Buschow, *Physica B + C* **128**, 265 (1985).

⁴L. Sun, J. Guo, G. Chen, X. Chen, X. Dong, W. Lu, C. Zhang, Z. Jiang, Y. Zou, S. Zhang *et al.*, *Phys. Rev. B* **82**, 134509 (2010).

⁵J. C. Cooley, M. C. Aronson, J. L. Sarrao, and Z. Fisk, *Phys. Rev. B* **56**, 14541 (1997).

⁶J. R. Shannon and M. J. Sienko, *Inorg. Chem.* **11**, 904 (1972).

⁷C. Guy, S. von Molnar, J. Etourneau, and Z. Fisk, *Solid State Commun.* **33**, 1055 (1980).

⁸G. Schütz, W. Wagner, W. Wilhelm, P. Kienle, R. Zeller, R. Frahm, and G. Materlik, *Phys. Rev. Lett.* **58**, 737 (1987).

⁹J. C. Lang and G. Srajer, *Rev. Sci. Instrum.* **66**, 1540 (1995).

¹⁰A. Dadashev, M. P. Pasternak, G. K. Rozenberg, and R. D. Taylor, *Rev. Sci. Instrum.* **72**, 2633 (2001).

¹¹K. Syassen, *High Press. Res.* **28**, 75 (2008).

¹²D. Haskel, Y. C. Tseng, J. C. Lang, and S. Sinogeikin, *Rev. Sci. Instrum.* **78**, 083904 (2007).

¹³P. Blaha, K. Schwarz, G. Madsen, D. Kvasnicka, and J. Luitz, *WIEN2k, An Augmented Plane Wave + Local Orbitals Program for Calculating Crystal Properties* (Technische Universität Wien, 2001).

¹⁴J. C. Lang, G. Srajer, C. Detlefs, A. I. Goldman, H. König, X. Wang, B. N. Harmon, and R. W. McCallum, *Phys. Rev. Lett.* **74**, 4935 (1995).

¹⁵R. F. Pettifer, S. P. Collins, and D. Laundy, *Nature (London)* **454**, 196 (2008).

¹⁶N. M. Souza-Neto, D. Haskel, Y.-C. Tseng, and G. Lapertot, *Phys. Rev. Lett.* **102**, 057206 (2009).

¹⁷R. T. Lechner, G. Springholz, T. U. Schüllli, J. Stangl, T. Schwarzl, and G. Bauer, *Phys. Rev. Lett.* **94**, 157201 (2005).

¹⁸P. W. Anderson, *Phys. Rev.* **79**, 350 (1950).

¹⁹T. Kasuya, *Prog. Theor. Phys.* **16**, 45 (1956).

²⁰K. Yosida, *Phys. Rev.* **106**, 893 (1957).

²¹M. A. Ruderman and C. Kittel, *Phys. Rev.* **96**, 99 (1954).

²²D. Haskel, Y. B. Lee, B. N. Harmon, Z. Islam, J. C. Lang, G. Srajer, Y. Mudryk, K. A. Gschneidner, and V. K. Pecharsky, *Phys. Rev. Lett.* **98**, 247205 (2007).